Noise Analysis for Optical Fiber Communication Systems*

Alper Demir

aldemir@ku.edu.tr
Department of Electrical & Electronics Engineering
Koç University, Istanbul, Turkey

Abstract

The optical fiber transmission links form the backbone of the communications infrastructure. Almost all of voice and data (internet) traffic is routed through terrestrial and submarine optical fiber links, connecting the world together. Invention of the optical amplifiers (OAs) and wavelength-division multiplexing (WDM) technology enabled very high capacity optical fiber communication links that run for thousands of kilometers without any electronic repeaters, but at the same time brought many design challenges. As electronic amplifiers do, OAs add noise to the signal they amplify. In the design of an optical fiber communication link, the prediction of the deterioration the information signals experience due to the nonlinearity of the optical fiber and the optical noise generated by the OAs is essential. In this paper, we first present a short overview of optical fiber communication systems and the challenges that faces one from a modeling, analysis and design perspective. Then, we describe novel formulations and computational techniques for the analysis of the interplay between the information signals and the optical noise due to the fiber nonlinearity as they propagate together along the fiber link. Our formulations are similar, in spirit, to the linear(ized), time-varying formulations for noise analysis in analog/RF electronic circuits. We then investigate signal-noise mixing due to optical fiber nonlinearities using the techniques developed. Finally, we discuss the use of the generated results in the performance evaluation of communication links, and comment on system design implications.

1 Introduction

The optical fiber transmission links form the backbone of the communications infrastructure. Almost all of voice and data (internet) traffic is routed through terrestrial and submarine optical fiber links, connecting the world together. Invention of the optical amplifiers (OAs) and wavelength-division multiplexing (WDM) technology enabled very high capacity optical fiber communication links that run for thousands of kilometers without any electronic repeaters, but at the same time brought many design challenges.

In WDM optical fiber communications, information bits are used to modulate the (light) carriers at many wavelengths, which are then transmitted in a single strand of fiber. The signal levels deteriorate during transmission due to the loss of the optical fiber, which need to be restored by OAs for reliable detection. OAs have very wide bandwidths, e.g., 4 THz, they can amplify many wavelength carriers at once. As electronic amplifiers do, OAs add noise (∼white and stationary) to the signal they amplify. A long-haul optical fiber communication link may be several thousands of kilometers long, and it may have tens of optical amplification sites placed at regular intervals (∼ 80 km) along the link, as shown in Figure 1. The information signals in a number of WDM channels and the noise added by the OAs travel together in the optical fiber and impinge on the electronic receiver. The optical fiber is a lossy, dispersive, and *nonlinear* transmission medium. Due to the nonlinearity of the fiber, the information signals at different wavelengths and noise added by the OAs mix with each other as they propagate together along the fiber. The propagation of the signals and noise in an optical fiber is governed by a *nonlinear* partial differential equation (PDE), the so-called generalized nonlinear Schrödinger equation (**NLSE**), which can be derived directly from Maxwell's equations that govern the propagation of light waves in a dielectric waveguide, i.e., the optical fiber.

In the design of an optical fiber communication link, it is essential to be able to predict the deterioration the information signals experience due to the dispersion and nonlinearity of the optical fiber, and the optical noise generated by the OAs. In this paper, we focus on the analysis of the mixing of the information signals with noise, as opposed to the mixing of the information signals with each other, due to the fiber nonlinearity.

The mixing of the information signals with each other is also of great importance in systems design. We touch upon this phenomenon on several occasions in the paper, but a detailed treatment of signal-signal mixing analysis is beyond the scope of this work. There has been considerable effort and tremendous progress made on this problem in the literature. However, the need for more efficient, *semi-analytical* analysis techniques is still there.

Commonly, the prediction of noise-signal mixing is performed with a *Monte Carlo*-type propagation simulation, where the information signals and randomly generated optical noise are simulated together in a numerical solution of the **NLSE**. This kind of simulation is inefficient, because one needs to repeat the simulation for sufficiently many sample paths of the noise process. It also is incapable of providing systems design intuition. In a Monte-Carlo type simulation, one simulates signal-signal and signal-noise mixing together, which hides the separate and quite different performance degradation mechanisms due to these mixing processes. The "separated" analysis of these mechanisms, in fact, provides valuable systems design intuition, as we will demonstrate in this paper.

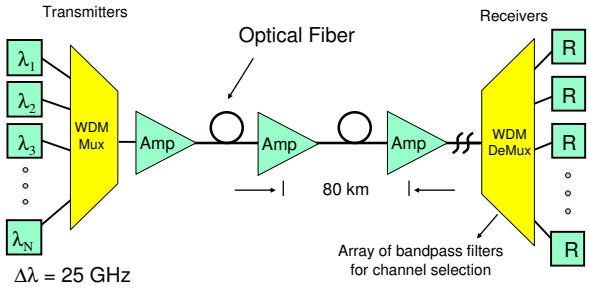

Figure 1: WDM optical fiber communication link

There has also been analytical approaches to the noise-signal mixing analysis problem in optical fiber propagation, and considerable progress has been made. It was first investigated in 1990 by Gordon and Mollenauer [1]. In their original treatment, they considered a system with a *single unmodulated* carrier, and *ignored dispersion* in the fiber. The dispersion in the fiber is of paramount importance in the analysis of signal-noise mixing. Kikuchi [2] included dispersion in his analysis, but it was also restricted to a single unmodulated carrier. Poggiolini and Benedetto et. al. [3] considered a *multi-wavelength* system with *unmodulated* carriers and took dispersion into account in their innovative analytical approach.

In this paper, we consider the most general case, a *multi-wavelength* system with *modulated carriers* with dispersion included. The treatment of this most general case requires the concepts of *nonstationarity* and *frequency correlation* for stochastic processes, i.e., noise signals, which we will discuss later. In Section 2, we describe novel formulations for the analysis of the interplay, i.e., mixing, between the information signals, i.e., modulated light carriers, and the optical noise due to the fiber nonlinearity. As with many other nonlinear and nonstationary stochastic problems, the problem in hand is conceptually challenging and computationally complex. We try to alleviate these difficulties through the use of semi-analytical formulations and sophisticated numerical techniques for the computational problem. In this context, "semi-analytical" is used to mean that, even though the formulation itself is fully analytical, it does not yield to a closed-form solution, and still requires the numerical solution of (partial) differential equations. However, the equations that need to be solved are different, and involve different variables, compared with the ones solved with the *brute-force* Monte Carlo simulation approach. In particular, we use *linear(ized)* {*time,space*}*-varying, nonstationary* formulations. Our approach is similar, in spirit, to the linear(ized), time-varying formulations for noise analysis in analog/RF electronic circuits [4]. A linearization formulation was also used by Poggiolini et. al. [3].

For the numerical computation problem, we employ *linearly (diagonally)-implicit multistep* (not to be confused with implicit linear multistep) integration methods to solve the *stiff* systems of differential equations generated by our noise analysis formulations. We describe, in Section 3, these numerical methods and their practical implementation for optical fiber communication link analysis. Then, in Section 4, we present results generated by the proposed and implemented techniques in the investigation of signal-noise mixing due to the optical fiber nonlinearities. We discuss the use of the generated results in determining the performance of communication links, and discuss system design implications.

*This work was supported by a Turkish Academy of Sciences GEBIP fellowship.

ICCAD'03, November 11-13, 2003, San Jose, California, USA.

2 Formulations for linear(ized) noise analysis

The nonlinear Schrödinger equation that governs the evolution of the complex envelope $U(z,t)$ for the electric field in single-mode optical fibers [5] is given below

$$\frac{\partial U(z,t)}{\partial z} = -\frac{1}{2}\alpha U(z,t) - j\frac{1}{2}\beta_2\frac{\partial^2 U(z,t)}{\partial t^2} + \frac{1}{6}\beta_3\frac{\partial^3 U(z,t)}{\partial t^3} + j\gamma|U(z,t)|^2\,U(z,t) \tag{1}$$

where t is time, z is the position in the propagation direction along the fiber, α models the loss of the fiber (assumed frequency/wavelength independent here), the terms with β_2 and β_3 model 2nd and 3rd order dispersion (the effect of which is equivalent to an all-pass linear filter with phase distortion), and the term with γ models the nonlinearity of the fiber. First order dispersion β_1 has been factored out through a change of variable, since it amounts to a pure time delay, without any phase distortion. Values of the parameters for loss, dispersion and nonlinearity for various kinds of fibers are available. (1) can be derived directly from Maxwell's equations [5]. $U(z,t)$ is the *complex envelope* for the electric field. The *very* high frequency ($\sim$200 THz) lightwave carrier, as well as the transverse, i.e., $x-y$, electric field profile, have been factored out of (1) through some verified approximations [5]. $U(z,t)$ and (1) are normalized in such a way that $|U(z,t)|^2$ is the instantaneous optical power.

Next, we derive a linear PDE for noise analysis, and then in Section 2.2, we describe a covariance matrix formulation for stochastic noise characterization. We also have developed and implemented a frequency-decomposed formulation for noise analysis. This alternative formulation has some benefits, its implementation can be parallelized for efficiency, and we have further developed it into a reduced-order-modeling formalism. Unfortunately, we are forced to skip the description of this formulation here due to space limitations and the prohibitive cost of the excess page fees.

2.1 Derivation of linear PDE for noise analysis

Let $A(z,t)$ be the solution of (1) without any noise in the system. Hence $A(z,t)$ satisfies (1). We describe the numerical computation of $A(z,t)$ in Section 3. $A(z=0,t)$ is the signal launched into the fiber. Note here that we do *not* place a restriction on the launched signal $A(0,t)$[1]. Now, we consider the system *with* noise and substitute $U(z,t) = A(z,t) + a(z,t)$ in (1)

$$\frac{\partial\,[A(z,t)+a(z,t)]}{\partial z} = -\frac{1}{2}\alpha\,[A(z,t)+a(z,t)] - j\frac{1}{2}\beta_2\frac{\partial^2[A(z,t)+a(z,t)]}{\partial t^2} + \frac{1}{6}\beta_3\frac{\partial^3[A(z,t)+a(z,t)]}{\partial t^3} + j\gamma|[A(z,t)+a(z,t)]|^2\,[A(z,t)+a(z,t)] \tag{2}$$

where $a(z,t)$ is a perturbation to $A(z,t)$ due to the noise of the OAs. We now subtract (1),with $U(t,z)$ replaced by $A(z,t)$, from (2) and obtain

$$\frac{\partial\,a(z,t)}{\partial z} = -\frac{1}{2}\alpha\,a(z,t) - j\frac{1}{2}\beta_2\frac{\partial^2 a(z,t)}{\partial t^2} + \frac{1}{6}\beta_3\frac{\partial^3 a(z,t)}{\partial t^3} + j\gamma|[A(z,t)+a(z,t)]|^2\,[A(z,t)+a(z,t)] - j\gamma\,|A(z,t)|^2\,A(z,t) \tag{3}$$

For linear(ized) noise analysis, we ignore all terms in (3) that are not linear in $a(z,t)$, justified by the fact that $a(z,t)$ is much "smaller" than $A(z,t)$, otherwise, the communication link is not useful.

$$\frac{\partial\,a(z,t)}{\partial z} = -\frac{1}{2}\alpha\,a(z,t) - j\frac{1}{2}\beta_2\frac{\partial^2 a(z,t)}{\partial t^2} + \frac{1}{6}\beta_3\frac{\partial^3 a(z,t)}{\partial t^3} + 2\,j\gamma\,|A(z,t)|^2\,a(z,t) + j\gamma A(z,t)^2\,a(z,t)^\star \tag{4}$$

where * denotes "complex-conjugate". In (4), $a(z,t)$ is a complex-valued scalar function of z and t. We decompose $a(z,t)$ into its real (in-phase) and imaginary (quadrature) components

$$a(z,t) = a_r(z,t) + j\,a_i(z,t) \qquad A(z,t) = A_r(z,t) + j\,A_i(z,t) \tag{5}$$

[1]Authors in [3] assume that $A(0,t)$ is a *comb* of continuous-wave (CW), i.e., unmodulated, optical carriers. Moreover, with their formulation, they also ignore (four-wave) mixing among the carriers themselves.

With (5), (4) becomes

$$\frac{\mathrm{d}}{\mathrm{d}z}\begin{bmatrix}a_r(z,t)\\ a_i(z,t)\end{bmatrix} = -\frac{1}{2}\alpha\begin{bmatrix}a_r(z,t)\\ a_i(z,t)\end{bmatrix} + \frac{1}{2}\beta_2\begin{bmatrix}0 & \frac{\partial^2}{\partial t^2}\\ -\frac{\partial^2}{\partial t^2} & 0\end{bmatrix}\begin{bmatrix}a_r(z,t)\\ a_i(z,t)\end{bmatrix} + \frac{1}{6}\beta_3\begin{bmatrix}\frac{\partial^3}{\partial t^3} & 0\\ 0 & \frac{\partial^3}{\partial t^3}\end{bmatrix}\begin{bmatrix}a_r(z,t)\\ a_i(z,t)\end{bmatrix} + \gamma\begin{bmatrix}-2A_r(z,t)A_i(z,t) & -A_r(z,t)^2 - 3A_i(z,t)^2\\ 3A_r(z,t)^2 + A_i(z,t)^2 & 2A_r(z,t)A_i(z,t)\end{bmatrix}\begin{bmatrix}a_r(z,t)\\ a_i(z,t)\end{bmatrix} \tag{6}$$

In the linear(ized) PDEs (4) and (6) above, $A(z,t)$ is the deterministic multi-channel modulated optical signal, and $a(z,t)$ is the stochastic perturbation due to noise.

2.2 Covariance matrix formulation for noise analysis

We start by discretizing time t with N time points $t_1, t_2, \ldots, t_{N_t-1}, t_{N_t}$ which are not necessarily equispaced. We define the column vectors

$$\mathbf{a}_c(z) = [a(z,t_1) \quad a(z,t_2) \quad \cdots \quad a(z,t_{N_t})]^T \qquad \mathbf{A}_c(z) = [A(z,t_1) \quad A(z,t_2) \quad \ldots \quad A(z,t_{N_t})]^T \tag{7}$$

where the bold characters and the subscript c denote that $\mathbf{a}_c(z)$ and $\mathbf{A}_c(z)$ are complex-valued *vector* functions of z. The time dependence has disappeared because of the collocation points we have introduced. We separate $\mathbf{a}_c(z)$ and $\mathbf{A}_c(z)$ into their real and imaginary parts

$$\mathbf{a}_c(z) = \mathbf{a}_r(z) + j\,\mathbf{a}_i(z) \qquad \mathbf{A}_c(z) = \mathbf{A}_r(z) + j\,\mathbf{A}_i(z) \tag{8}$$

and form the real-valued long column vectors

$$\mathbf{a}(z) = \begin{bmatrix}\mathbf{a}_r(z)^T & \mathbf{a}_i(z)^T\end{bmatrix}^T \qquad \mathbf{A}(z) = \begin{bmatrix}\mathbf{A}_r(z)^T & \mathbf{A}_i(z)^T\end{bmatrix}^T \tag{9}$$

With (9), (6) turns into

$$\frac{\mathrm{d}\,\mathbf{a}(z)}{\mathrm{d}z} = -\frac{1}{2}\alpha\,\mathbf{a}(z) + \frac{1}{2}\beta_2\begin{bmatrix}0 & \mathbb{D}_2\\ -\mathbb{D}_2 & 0\end{bmatrix}\mathbf{a}(z) + \frac{1}{6}\beta_3\begin{bmatrix}\mathbb{D}_3 & 0\\ 0 & \mathbb{D}_3\end{bmatrix}\mathbf{a}(z) + \gamma\begin{bmatrix}-2\,\mathcal{D}[\mathbf{A}_r(z)]\,\mathcal{D}[\mathbf{A}_i(z)] & -\mathcal{D}[\mathbf{A}_r(z)]^2 - 3\,\mathcal{D}[\mathbf{A}_i(z)]^2\\ 3\,\mathcal{D}[\mathbf{A}_r(z)]^2 + \mathcal{D}[\mathbf{A}_i(z)]^2 & 2\,\mathcal{D}[\mathbf{A}_r(z)]\,\mathcal{D}[\mathbf{A}_i(z)]\end{bmatrix}\mathbf{a}(z) \tag{10}$$

where $\mathbb{D}_2$ and $\mathbb{D}_3$ are second-order and third-order differentiation operators (or matrices) in time, and $\mathcal{D}[\cdot]$ is a diagonal operator (or a diagonal matrix with the elements of the argument vector on the main diagonal). At this point, we do not make any assumptions on how the time differentiation operators $\mathbb{D}_2$ and $\mathbb{D}_3$ are implemented. We define

$$\mathbb{A}(z) = \begin{bmatrix}-2\,\mathcal{D}[\mathbf{A}_r(z)]\,\mathcal{D}[\mathbf{A}_i(z)] & -\mathcal{D}[\mathbf{A}_r(z)]^2 - 3\,\mathcal{D}[\mathbf{A}_i(z)]^2\\ 3\,\mathcal{D}[\mathbf{A}_r(z)]^2 + \mathcal{D}[\mathbf{A}_i(z)]^2 & 2\,\mathcal{D}[\mathbf{A}_r(z)]\,\mathcal{D}[\mathbf{A}_i(z)]\end{bmatrix} \tag{11}$$

$$\mathbb{B}_2 = \begin{bmatrix}0 & \mathbb{D}_2\\ -\mathbb{D}_2 & 0\end{bmatrix} \qquad \mathbb{B}_3 = \begin{bmatrix}\mathbb{D}_3 & 0\\ 0 & \mathbb{D}_3\end{bmatrix} \tag{12}$$

With (11) and (12), (10) turns into

$$\frac{\mathrm{d}\,\mathbf{a}(z)}{\mathrm{d}z} = -\frac{1}{2}\alpha\,\mathbf{a}(z) + \frac{1}{2}\beta_2\mathbb{B}_2\,\mathbf{a}(z) + \frac{1}{6}\beta_3\mathbb{B}_3\,\mathbf{a}(z) + \gamma\,\mathbb{A}(z)\,\mathbf{a}(z) \tag{13}$$

Now we form

$$\frac{\mathrm{d}\,[\mathbf{a}(z)\,\mathbf{a}(z)^T]}{\mathrm{d}z} = \frac{\mathrm{d}\,\mathbf{a}(z)}{\mathrm{d}z}\,\mathbf{a}(z)^T + \mathbf{a}(z)\,\frac{\mathrm{d}\,\mathbf{a}(z)^T}{\mathrm{d}z} \tag{14}$$

and let $\mathbf{K}(z)$ be the z-dependent *covariance matrix* for the time-collocated stochastic perturbation

$$\mathbf{K}(z) = \mathtt{E}\,[\mathbf{a}(z)\,\mathbf{a}(z)^T] \tag{15}$$

where $\mathtt{E}\,[\cdot]$ denotes the probabilistic "expectation" operator. Note that $\mathbf{K}(z)$ is a real and symmetric matrix. Then, we substitute (13) in (14), take the expectation of both sides, and obtain

$$\frac{\mathrm{d}\,\mathbf{K}(z)}{\mathrm{d}z} = -\alpha\,\mathbf{K}(z) + \frac{1}{2}\beta_2\Big[\mathbb{B}_2\,\mathbf{K}(z) + \mathbf{K}(z)\,\mathbb{B}_2^T\Big] + \frac{1}{6}\beta_3\Big[\mathbb{B}_3\,\mathbf{K}(z) + \mathbf{K}(z)\,\mathbb{B}_3^T\Big] + \gamma\Big[\mathbb{A}(z)\,\mathbf{K}(z) + \mathbf{K}(z)\,\mathbb{A}(z)^T\Big] \tag{16}$$

which is a system of *linear* differential equations for the *covariance matrix* of the time-collocated stochastic perturbation. We will refer to this equation as **COVODE** during the rest of our treatment. Note that even though $\mathbb{B}_2$ and $\mathbb{B}_3$ above do not depend on z, $\mathbb{A}(z)$ is a z-*varying* coefficient matrix which can be calculated by substituting $A(z,t)$ in (11). By solving the system of differential equations above, one can compute the noise covariance matrix $\mathbf{K}(z=L)$ at the end of the fiber link given an "initial" launch condition $\mathbf{K}(z=0)$. The numerical computation of $\mathbf{K}(z)$ is described in Section 3. Note that the stochastic perturbation $a(z,t)$ is, in general, a *nonstationary* stochastic process as a function of time t, which is captured by the covariance matrix formalism described above.

3 Numerical methods and implementation

In this section, we will describe the numerical solution of

- Equation (1) (**NLSE**) for the deterministic multi-channel modulated optical signal, in Section 3.1
- Equation (16) (**COVODE**) for the covariance matrix of the time-collocated noise, i.e., stochastic perturbation, in Section 3.2

3.1 Numerical solution of NLSE

(1) is a PDE which combines a low-order (zeroth) nonlinear term with higher-order (2nd and 3rd) linear terms. To obtain efficient and accurate numerical solutions for such PDEs, it is desirable to use high-order approximations in space z and time t [6]. Spectral methods offer very high *time* resolution for (1) [7, 8]. Once the time part of (1) is spectrally discretized and the resulting system of ordinary differential equations (ODEs) is transformed into the spectral domain, one obtains

$$\frac{\mathrm{d}}{\mathrm{d}z}\hat{\mathbf{A}}(z) = L\hat{\mathbf{A}}(z) + N\big[\hat{\mathbf{A}}(z)\big] \tag{17}$$

where N is a nonlinear operator, and L is a diagonal matrix (operator). L has widely varying values on the diagonal, since the diagonal elements are the summation of a quadratic and cubic function of the frequency variable (due to 2nd and 3rd order dispersion). Hence, the linear part of the system of ODEs in (17) is *stiff*. This stiffnes combined with the nonlinearity in (17) precludes the use of high-order schemes for z-integration because of severe stability restrictions [8, 6]. The stability restriction imposes an upper limit on the size of the z-steps that can be taken.

L in (17) (which is in the spectral domain) is diagonal and can be applied trivially. However, the nonlinear operator N in (17) needs to be implemented in the time-domain, this requires two FFTs, one to go back to the time-domain and another one to come back to the spectral domain. The nonlinear operator N is diagonal in the time-domain.

In the optical fiber communication community, the z-stepping method of choice is the so-called *split-step* method [7], an *explicit* z-stepping scheme based on operator splitting. When a sufficiently small step size is not used with this method, inaccuracies due to instability in numerical integration manifests itself as induced spurious tones, which are called *fictitious four-wave mixing* in the photonics literature [9].

If an *implicit* scheme is used for z-stepping, larger steps can be taken compared with an explicit scheme. However, even implicit z-stepping may suffer from (milder) stability restrictions on the step size when high-orders are used. One may be limited by a second-order A-stable scheme, e.g., trapezoidal formula. Moreover, an implicit scheme applied to (17) requires the solution of a *system of nonlinear equations* at every z-step.

The idea behind the *linearly-implicit* schemes [8, 6] arises from the observation that the stiffness in (17) is due to the *linear* part, and hence one can use an implicit (possibly A-stable) multi-step formula to advance the linear part and an explicit high-order scheme to advance the nonlinear part. Then, the step-size would become accuracy-limited and not stability-limited. Moreover, the solution of only a *linear* system of equations at every step would be needed. L in (17) is *diagonal* when time discretization is done with a spectral method, and hence the linear system of equations that need to be solved at every z-step is diagonal and has a trivial solution.

Fornberg and Driscoll [8] describe an extension of the linearly-implicit scheme above. In addition to applying separate explicit and implicit integration methods for the nonlinear and the linear part, they also split the linear part into *low, medium* and *high* Fourier wavenumber regions. These wavenumber regions correspond to *slow, medium* and *fast* time scales. In the *slider* method they propose, they use a different integration scheme for each (Fourier wavenumber) region in the linear part. For the low Fourier wavenumber region, they use the same explicit high-order scheme used for the nonlinear part. In one version of the slider method, Fornberg and Driscoll [8] use low:**AB7/AB7**, medium:**AB7/AM6** and high:**AB7/AM2*** for the (**nonlinear/linear** part where **ABk** is the explicit kth order Adams-Bashfort formula, and **AMk** is the implicit kth order Adams-Moulton formula. The diagonal linear term L in (17) has a complex spectrum with a very small real part compared with the imaginary part. The (frequency-independent) real part is due to the loss of the fiber, and the (strongly frequency-dependent) imaginary part is due to 2nd and 3rd order dispersion. The boundaries between the low, medium, and high Fourier wavenumber regions are determined by the extent of the stability regions along the imaginary axis for the integration schemes used for the linear part. **AM2*** above

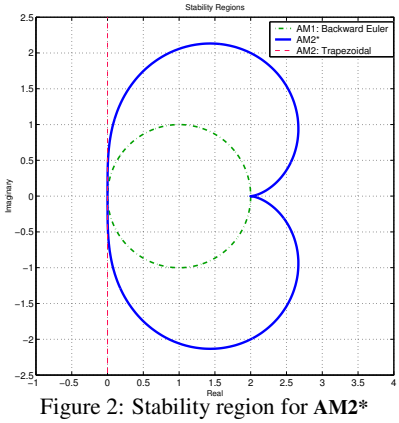

Figure 2: Stability region for **AM2***

is a modified second-order formula, which is given by

$$\hat{\mathbf{A}}_{n+1} - \hat{\mathbf{A}}_n = \frac{h}{2}\left(\frac{3}{2}L\hat{\mathbf{A}}_{n+1} + \frac{1}{2}L\hat{\mathbf{A}}_{n-1}\right) \tag{18}$$

when constant step sizes are used, with h as the z-step size [8]. Note that (18) is a *two-step* second-order formula in contrast with the one-step second-order **AM2** (trapezoidal rule). It has an error constant of $\frac{1}{3}$ compared with $\frac{1}{12}$ for **AM2**. However, its stability region (Figure 2) extends into the right-half-plane covering the imaginary axis. Fornberg and Driscoll [8] propose **AM2*** in place of **AM2** for problems with almost a purely imaginary spectrum.

We have implemented a self-starting, fully-variable step size version of Fornberg and Driscoll's linearly-implicit slider method outlined above for the numerical solution of (1):**NLSE** for the deterministic multi-channel modulated optical signal. Automatic step size control is performed based on an estimation of the local truncation error [10]. Commonly used step size selection heuristics [10], as well as new ones we found to be useful that are specific to the linearly-implicit slider scheme described above, have been implemented in our code. The new heuristics are involved with the coordination of truncation error computation and step size selection in the presence of different integration schemes being used for the linear and nonlinear parts of (17) and also for the low, medium and high Fourier wavenumber regions of the linear part.

The numerical solution of **NLSE** has a computational complexity of $O(N_z N_f \log N_f)$, where N_f is the number of Fourier modes used in the spectral representation, and N_z is the number of z-steps. The storage complexity is $O(N_f)$.

For a comparison of the split-step method and the linearly-implicit schemes as well as other integration schemes for solving stiff nonlinear PDEs of the form in (17), please see [8, 6].

3.2 Numerical solution of COVODE

In contrast with the nonlinear **NLSE**:(1), **COVODE**:(16) is a linear system of equations. The right-hand-side (RHS) of **COVODE** has terms which have z-independent coefficient matrices. These arise from the linear loss and dispersion terms in the original **NLSE**. RHS of **COVODE** also has terms with z-dependent coefficient matrices. These terms arise from the nonlinear term in the original **NLSE**. **COVODE** is closely related to **NLSE**, and the same stiffness properties carry over. Hence, we use the same linearly-implicit slider schemes (described above) for the numerical integration of **COVODE**. In the context of **COVODE**, it is not exactly accurate to call the integration schemes as linearly-implicit, because all terms in **COVODE** are linear. To be precise, we use implicit sliding schemes for the medium and high wavenumber loss and dispersion terms in **COVODE**, and use explicit high-order, e.g., **AB7**, schemes for the low wavenumber loss and dispersion terms and the z-varying linear terms due to the nonlinearity of the fiber. Application of the "linearly" implicit integration schemes to **COVODE** in (16) is straightforward, except for some tinkering required on how to apply the sliding scheme with a partition of slow, medium and fast time scales.

We solve **COVODE** in (16) using the same spectral discretization for time t that we use for **NLSE**. We first transform (16) into the spectral domain. Then, the coefficient matrices $\mathbb{B}_2$ and $\mathbb{B}_3$ are given by (12) where $\mathbb{D}_2$ and $\mathbb{D}_3$ are now diagonal matrices.

For **COVODE**, we use the same z-stepping scheme and the same z-steps that is used and automatically selected for **NLSE**. At every z-step, we first compute the solution of **NLSE**, $\mathbf{A}_c(z) = \mathbf{A}_r(z) + j\,\mathbf{A}_i(z)$, which is needed to evaluate the z-varying coefficient matrix $\mathbb{A}(z)$ for

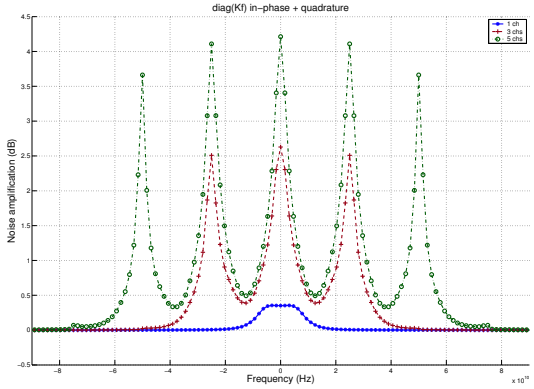

Figure 3: Unmodulated carriers, diag($\mathbf{K}_f$):in-phase+quad.

COVODE in (11). In the spectral domain, the evaluation of the term involving $\mathbb{A}(z)$ in **COVODE** requires the use of FFTs. When we apply an explicit multistep scheme to the z-varying terms involving $\mathbb{A}(z)$ in **COVODE**, and an implicit scheme to the loss and dispersion terms involving α, $\mathbb{D}_2$ and $\mathbb{D}_3$, we need to solve a matrix equation, at every z-step, of the form given by

$$\mathbf{E}\,\mathbf{K}_f(z_n) + \mathbf{K}_f(z_n)\,\mathbf{E}^\dagger = \mathbf{F}(z_n) \tag{19}$$

where † denotes conjugate-transpose, and

$$\mathbf{E} = \begin{bmatrix} \mathbf{D}_d & \mathbf{D}_o \\ -\mathbf{D}_o & \mathbf{D}_d \end{bmatrix} \tag{20}$$

where $\mathbf{D}_d$ and $\mathbf{D}_o$ are z-independent diagonal matrices. The subscript $_f$ for $\mathbf{K}_f(z_n)$ denotes that we are in the spectral domain. (19) is a Lyapunov matrix equation [11]. A direct-method solution of the Lyapunov matrix equation using the Bartels-Stewart algorithm is $O(N_f^3)$ [12]. However, since the coefficient matrix $\mathbf{E}$ is in a very special form, we do not need to use the Bartels-Stewart algorithm which is meant to handle arbitrary coefficient matrices. When $\mathbf{E}$ is in the form given by (20), (19) can be solved with a specialized algorithm that is $O(N_f^2)$, the description of which we are forced to skip due to space limitations.

With a flat and unstructured representation for the covariance matrix, it is not possible to reduce the computational complexity of the solution of (19) below $O(N_f^2)$. If the stochastic perturbation is a stationary process, then the covariance matrix in the spectral domain is diagonal, and in the time domain it is Hermitian and Toeplitz[2]. Hence, it is structured and can be represented with $O(N_f)$ numbers as opposed to $O(N_f^2)$ numbers. However, in general, the stochastic perturbation is nonstationary, and there is no apparent exact structure in the covariance matrix. Still, it is worthwhile to investigate if there is any (numerically approximate) special structure that arises in the noise covariance matrices and how it can be exploited for efficient representation and computation. With an unstructured, flat representation for the covariance matrix, the computational complexity for the numerical solution of **COVODE** is $O(N_z N_f^2 \log N_f)$, the storage complexity is $O(N_f^2)$.

We have implemented the above outlined method for the numerical solution of **COVODE**:(16) along with the numerical solution of **NLSE**:(1). Noise analysis examples generated using this implementation and a discussion of system performance evaluation using the noise analysis results is in Section 4.

4 Noise analysis examples and discussion

System model

For the noise analysis examples we are going to present in this section, we use the model of an optical fiber communication link like the one shown in Figure 1. The frequency separation between channels was set to 25 GHz. The span length between amplifier sites was set to 80 km. In the link of Figure 1, there is an OA before the first span of fiber. This OA sets the launch power for the channels, which was chosen as 10 mW/channel for all of the simulations that we will present. The WDM signal is launched into the link with the noise added by the first OA. The OAs along the link compensate for the loss of one span of fiber. They amplify the signal channels as well as the optical noise (which was added by the previous OAs along the link and "modified" by the fiber nonlinearity). The parameters used for the single-mode fiber were: $\alpha = 0.25$ dB/km, $\beta_2 = -21.6\,\mathrm{ps}^2/\mathrm{km}$, $\beta_3 = 0.128\,\mathrm{ps}^3/\mathrm{km}$, $\gamma = 1.2\,\mathrm{W}^{-1}.\mathrm{km}^{-1}$. Thus, the loss of a fiber span with a length of 80 km is 20 dB. Hence, the OAs in the link have a power gain of 20 dB. The noise added by the OAs is modeled as a complex (with uncorrelated in-phase and quadrature components), white (constant spectral density) and stationary (constant power, i.e., variance, as a function of time) process. The channel-combining and channel-selection bandpass filters in the WDM multiplexer and WDM demultiplexer were assumed to be ideal brick-wall filters.

For all of the examples we will present, number of Fourier modes for spectral time discretization N_f was set to 256, and 16 bits that repeat periodically were used in random pulse streams. The number of z-steps N_z depends on the truncation error tolerances and the frequency content of the signals being simulated. For signals with rich content in higher frequencies, smaller z-steps are required. For the simulations we performed, N_z ranged in 400-4000 for an 80 km length of fiber.

Fiber without nonlinearity

If the fiber has no nonlinearity, the noise analysis becomes trivial, because no signal-noise mixing occurs. The dispersion in the fiber still causes (linear) distortion to the signal channels. However, the second-order stochastic properties, i.e., the spectral density, of optical noise is *not* affected, because dispersion is equivalent to an all-pass filter with phase distortion. When a stochastic process passes through such a filter, its spectral properties remain unchanged. Thus, without nonlinearity, the optical noise at the end of link, impinging on the receiver, is still stationary and white. The contribution from each OA to the total accumulated optical noise at the end of the link is the same, because the OAs compensate for the loss of one span of fiber. The optical noise from different OAs is assumed to be uncorrelated with each other.

Fiber without dispersion, and a single unmodulated carrier

The noise analysis for this very special case can be performed analytically, as was done by Gordon and Molleanuer [1]. In this case, optical noise (quadrature component with respect to the carrier) experiences (uncolored) amplification but stays white, and also stationary (assuming that the complex envelope in **NLSE** is centered at the single unmodulated carrier). We compared the numerical results we obtained with our noise simulator with the analytical results[3] in [1], and as expected, the agreement is exact.

Stationary vs nonstationary, white vs colored noise

Stationary noise is characterized by a time-domain covariance matrix $\mathbf{K}_t$ which is Hermitian and Toeplitz. In the spectral domain, the covariance matrix is diagonal, indicating that there is no *spectral correlation*. The spectral domain covariance matrix for nonstationary noise is non-diagonal, and in the time-domain, it is not Toeplitz. For instance, the values on the main diagonal (i.e., the variance or noise power as a function of time) of the time-domain covariance matrix are not equal for nonstationary noise. From now on and in the figures that will follow, we will use $\mathbf{K}_f$ to indicate the spectral domain covariance matrix, and $\mathbf{K}_t$ for the time-domain covariance matrix. Please recall that $\mathbf{K}_t$ is the covariance matrix for the time samples of optical noise, and both $\mathbf{K}_t$ and $\mathbf{K}_f$ are a function of z, the position along the fiber link. White noise is characterized by a diagonal $\mathbf{K}_t$ (indicating no correlation between the time samples of noise) and a Hermitian Toeplitz $\mathbf{K}_f$. Notice that this characterization is the *dual* of the characterization for stationary noise described above. Colored noise has a non-diagonal $\mathbf{K}_t$ and hence a non-Toeplitz $\mathbf{K}_f$. Note that white noise is not necessarily stationary. We can now deduce that white and stationary noise has a diagonal $\mathbf{K}_f$ and diagonal $\mathbf{K}_t$ with constant entries on the diagonal[4]. The model that we use for the noise added by the OAs is white and stationary.

Comb of unmodulated carriers

We first present noise analysis results for the case of unmodulated carriers. We simulated a system like in Figure 1 with 1, 3 and 5 WDM channels. Figure 3 shows the main diagonal of $\mathbf{K}_f$ for the optical noise before the bandpass channel select filter (WDM demux) in the receiver. $\mathbf{K}_f$ in all of the figures we are going to present is normalized with the $\mathbf{K}_f$ one would obtain without any nonlinearity in the fiber. Hence, the y-axis in all of $\mathbf{K}_f$ plots represents *noise amplification* (in dBs) due to signal-noise mixing. In Figure 3, the total noise power,

[2] A Toeplitz matrix is a matrix whose entries are constant on each diagonal.

[3] The results in [1] are approximate if the number of spans is not large, and they need to be modified to become exact for few spans.

[4] Hermitian, Toeplitz and diagonal matrix = a scalar multiple of the identity matrix.

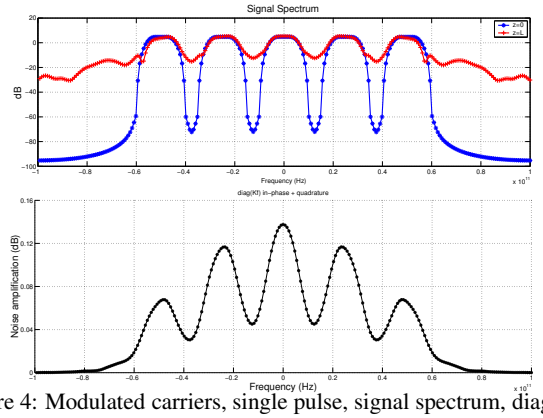

Figure 4: Modulated carriers, single pulse, signal spectrum, diag($\mathbf{K}_f$)

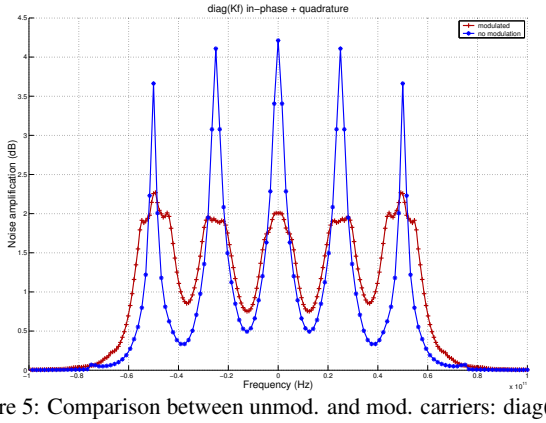

Figure 5: Comparison between unmod. and mod. carriers: diag($\mathbf{K}_f$)

total for the in-phase and quadrature components, is shown. For the 5-channel case, the noise amplification at the carrier frequencies reaches ~ 4 dB. It decreases rapidly as one moves away from the carrier frequencies. This decrease is due to dispersion in the fiber. Without dispersion, the noise amplification would have been uncolored, constant for all frequencies and equal to the value at $f = 0$. Hence, without dispersion, the effects of signal-noise mixing would have been *disastrous*. Moreover, as observed in Figure 3, the increase in noise amplification (away from the carriers) from the 1-channel to the 3-channel case is more than the increase from the 3-channel case to the 5-channel one. This means that signal-noise mixing due to nearby channels is more severe than the noise-signal mixing due to channels further away. This is again due to dispersion. Without dispersion, the noise-signal mixing severity would be independent of the frequency separation between channels. The above is true only for noise amplification away from the carrier frequencies. The noise amplification at the carrier frequencies is not affected by dispersion and increases severely as the number of channels increase. In fact, the noise amplification at the carrier frequencies is directly proportional to the number of channels. However, the noise amplification away from the carrier frequencies has a much milder dependence on the number of channels and does not increase much more as the number of channels is increased. With unmodulated carriers, the noise before the WDM demux is *nonstationary*, however it becomes stationary *after* the bandpass channel select filter.

Carriers modulated with a single pulse

We now present noise analysis results when the carriers are modulated with a single pulse. Upper plot in Figure 4 shows the spectrum of the signal launched into the fiber, and also the signal spectrum at the end of the span. Bottom plot in Figure 4 is the main diagonal of $\mathbf{K}_f$ before the channel select filter.

Carriers modulated with random pulse stream

We will now compare the noise analysis results for unmodulated carriers and carriers modulated with a random pulse stream. Figure 5 shows diag($\mathbf{K}_f$) for unmodulated and random pulse stream modulated carriers, both before the channel select filter. The average carrier power was kept equal for the two cases. We observe that, with modulation, the magnitude of noise amplification at the carrier frequency decreases. However, the noise amplification at frequencies away from, and in-between, the carriers increases. The total integrated noise power is approximately equal for these two cases. If we focus on the noise spectrum for the channel of interest centered at $f = 0$, there is more noise power in high frequencies in the modulated case compared with the unmodulated one. This, in time domain, corresponds to a *smaller* correlation width for noise. In other words, if noise is sampled at the bit rate, then two consecutive samples will have a larger correlation in the unmodulated case compared with the modulated one.

System design implications and performance evaluation

The results we obtained above using the noise analysis methodology we developed and implemented have significant design implications, and can be used in system performance (BER) evaluations, which we briefly outline and summarize next.

Dispersion plays a significant role in the process of signal-noise mixing. The effects of noise-signal mixing would be *disastrous* without dispersion in the fiber.

With dispersion and nonlinearity in the fiber, the optical noise experiences colored amplification due to signal-noise mixing, as seen in Figure 5. Amplification is more severe around the carrier frequencies and it is proportional to the number of channels. Amplification away from the carrier frequencies is much smaller and has a very mild dependence on the number of channels. The optical noise sampled at the bit rate in the receiver has much larger power (compared with the case without signal-noise mixing) but the consecutive samples of noise becomes highly correlated due to low-frequency enhanced colored amplification. However, the correlation between consecutive samples is not as large as one would predict with unmodulated carriers. The modulation of the carriers results in a relatively smaller amplification of low (around the carriers) frequency noise and a relatively larger amplification of high (around the midpoint between the carriers) frequency noise. The correlation between consecutive noise samples can be used to guide the selection of the modulation scheme in system design. For instance, modulation schemes which encode data *differentially* between two samples at the bit rate can make use of the correlation between the noise samples to improve BER performance in the presence of signal-noise mixing. Without signal-noise mixing, the optical noise stays white and the consecutive noise samples are uncorrelated.

The full stochastic characterization, including all correlation information, of optical noise samples at the receiver is available from the noise covariance matrices that our analysis techniques produce. This information can be used in BER performance evaluation.

5 Future work

More efficient numerical methods and z-stepping strategies for NLSE, a parallelized and/or reduced-order-modeling based implementation of the frequency-decomposed formulation mentioned in Section 2, investigation of efficient special-structure-exploiting representations for the noise covariance matrices, as well as the use and application of the noise analysis techniques developed in this paper in the design of signal-noise-mixing immune modulation schemes and system BER estimation is part of the future work. We plan to include the implementations of the numerical techniques described in the paper in an analysis and design tool for optical fiber communication links.

Acknowledgments

The author would like to thank Professor Jacob White and his group at MIT for hosting him during Summer 2002.

References

[1] J. P. Gordon and L. F. Mollenauer. Phase noise in photonic communication systems using linear amplifiers. *Optics Letters*, 15(23):1351, December 1990.

[2] K. Kikuchi. Enhancement of optical-amplifier noise by nonlinear refractyive index and group-velocity dispersion of optical fibers. *IEEE Photonics Technology Letters*, 5(2):221, February 1993.

[3] G. Bosco, A. Carena, V. Curri, R. Gaudino, P. Poggolini, and S. Benedetto. Parametric gain in multiwavelength systems: A new approach to noise enhancement analysis. *IEEE Photonics Technology Letters*, 11(9):1135, September 1999.

[4] A. Demir and A. Sangiovanni-Vincentelli. *Analysis and Simulation of Noise in Nonlinear Electronic Circuits and Systems*. Kluwer Academic Publishers, 1998.

[5] G. P. Agrawal. *Nonlinear Fiber Optics*. Academic Press, 1995.

[6] A. K. Kassam and L. N. Trefethen. Fourth-order time-stepping for stiff pdes. *SIAM J. Sci. Comp.*, submitted: http://web.comlab.ox.ac.uk/oucl/work/nick.trefethen/etd.ps.gz.

[7] L. N. Trefethen. *Spectral methods in* MATLAB. SIAM:Philadelphia, 2000.

[8] B. Fornberg and T. A. Driscoll. A fast spectral algorithm for nonlinear wave equations with linear dispersion. *J. Comp. Phys.*, (155):456–467, 1999.

[9] G. Bosco, A. Carena, V. Curri, R. Gaudino, P. Poggolini, and S. Benedetto. Supression of spurious tones induced by the split-step method in fiber systems simulation. *IEEE Photonics Technology Letters*, 12(5):489, May 2000.

[10] E. Hairer, S. P. Norsett, and G. Wanner. *Solving Ordinary Differential Equations I: Nonstiff Problems*. Springer-Verlag: Berlin Heidelberg, second revised edition, 1993.

[11] A.S. Hodel and S.T. Hung. Solution and applications of the lyapunov equation for control systems. *IEEE Transactions on Industrial Electronics*, 39(3):194, June 1992.

[12] R.H. Bartels and G.W. Stewart. Solution of the equation $ax + xb = c$. *Commun. ACM*, 15:820–826, 1972.